UDC 519.61:624.04:624.073
Original scientific paper
Received: 26.06.2003.

Thin plate quadrilateral element with independent rotational DOF

Željana Nikolić and **Ante Mihanović**
University of Split, Faculty of Civil Engineering, Matice hrvatske 15, HR-21000 Split, CROATIA
e-mail: Zeljana.Nikolic@gradst.hr, Ante.Mihanovic@gradst.hr

SUMMARY

This paper presents a quadrilateral thin plate bending element with a full compatibility of displacements and rotations at the nodes. A four-node finite element with independent translational and rotational degree of freedom (DOF) at each node is used. The shape functions for the approximation of the displacements and rotations are different and they are both determined from a complete polynomial of the fourth order. After satisfying conditions for the value of the functions and their first derivations at the element nodes, the shape functions consist of a fixed part satisfying the homogeneous differential equation and additional modes. The first one ensures high accuracy of the solution for the finite element with parallel opposite sides (rectangular, parallelogram). The additional modes in the shape functions of the rotational angle can be used for improving a solution in an arbitrarily quadrilateral finite element mesh. Described procedures ensure a high order of interpolation for the plate displacement. In both cases finite element possesses twelve global degrees of freedom. The additional unknowns in the rotational shape functions of an arbitrarily quadrilateral element are eliminated on the element level.

Key words: *thin plate, quadrilateral finite element, independent rotational DOF.*

1. INTRODUCTION

The finite element models based on the displacement method are very popular in engineering. However, thin plate bending elements [1, 2] based on the Kirchhoff theory may cause unconvergence problems due to C^1 continuity requirement. Quadrilateral displacement element with 12 degrees of freedom (DOF) based on a polynomial expression does not satisfy the C^1 continuity requirement. Therefore, 12 DOF plate element based on the displacement method with the weaker continuity requirement, called a non-conforming element [3, 4], has become a challenge to many researches.

Many alternative ways for improving the behaviour of quadrilateral thin plate elements in distorted mesh have been developed. The most significant of them are: hybrid stress element [5], discrete Kirchhoff element [6], generalized conforming element [7] and refined non-conforming element [8].

An alternative way is modelling based on the Reissner-Mindlin theory instead of Kirchhoff theory. In this case only C^0 shape function continuity is required, hence an interpolation field is more easily constructed. In most plate elements using Reissner-Mindlin assumptions, the interpolation used for the transversal displacements and the rotations involves the independent representation of each variable by its nodal values, usually with identical interpolations. To ensure a higher order of expansion for displacement, the concept of linked interpolation [9] of the displacement and rotations is introduced. In the context of the thick plate, quadrilateral elements employing linked interpolation have been developed in Refs. [10-12].

An independent representation of translational and rotational field and linking them can be also used for improving the accuracy and convergence of a quadrilateral thin plate element.

This paper presents a quadrilateral four-node thin plate bending element with a full compatibility of displacements and rotations at the nodes. The element has independent translational and rotational degrees of freedom at each node. This is in accordance with a unified approach to structural system modelling [13]. A similar element with independent translational and rotational DOF and Hermitian shape functions has been developed in Ref. [14].

The shape functions for the approximation of the displacement field in this paper are determined from a complete polynomial of the fourth order. The different interpolation is used for the translational and rotational part of the displacement field. After satisfying the conditions for the value of the functions and their first derivations at element nodes, shape functions consist of a fixed part satisfying the homogeneous differential equation and additional internal modes. Two types of shape functions are tested on examples with a regular and irregular finite element mesh: the shape functions which satisfy the homogeneous differential equation of the thin plate bending (SF1) and the shape functions with additional internal modes in the functions of rotational angle which depend on the finite element geometry (SF2).

2. APPROXIMATION OF THE DISPLACEMENT FIELD

The displacement field $\boldsymbol{p}$ of the loaded plate, according to the thin plate theory, is determined if the deflection of the plate $\boldsymbol{w}$ is known at all points. The displacement field can be represented according to the equation:

$$\boldsymbol{p} \equiv \boldsymbol{w} = \boldsymbol{N}\boldsymbol{u} = [\boldsymbol{N}_1, \boldsymbol{N}_2, \ldots, \boldsymbol{N}_n] \begin{bmatrix} \boldsymbol{u}_1 \\ \boldsymbol{u}_2 \\ \vdots \\ \boldsymbol{u}_n \end{bmatrix} \qquad (1)$$

where $\boldsymbol{N}$ is the matrix of shape functions and $\boldsymbol{u}$ is the vector of nodal displacement.

In this paper the finite elements with three degrees of freedom independent of each other are used, one translational displacement w_i perpendicular to the plate mid-plane and two rotational angles φ_i and θ_i around two orthogonal axes located at the plate mid-plane. The unknown displacement vector $\boldsymbol{u}_i$ at each node i ($i=1, \ldots, n$) of the plate element and the corresponding vector of the shape functions $\boldsymbol{N}_i$ can be represented as follows:

$$\boldsymbol{u}_i = [w_i, \varphi_i, \theta_i]^T, \quad \boldsymbol{N}_i = [n_{iw}, n_{i\varphi}, n_{i\theta}] \qquad (2)$$

where n_{iw} is the shape function with a unit translational displacement at the *i-th* node, while $n_{i\varphi}$ and $n_{i\theta}$ are the shape functions with a unit rotational angle around axes ξ and η, respectively.

The shape functions for the approximation of the displacement field n_{ij} ($i=1,\ldots,4$; $j=w,\varphi,\theta$) are determined from a complete polynomial of the forth order with 15 terms:

$$\begin{aligned} n_{ij} &= c_1 + c_2\xi + c_3\eta + c_4\xi^2 + c_5\xi\eta + c_6\eta^2 + \\ &+ c_7\xi^3 + c_8\xi^2\eta + c_9\xi\eta^2 + c_{10}\eta^3 + c_{11}\xi^4 + \\ &+ c_{12}\xi^3\eta + c_{13}\xi^2\eta^2 + c_{14}\xi\eta^3 + c_{15}\eta^4 \end{aligned} \qquad (3)$$

The shape functions associated with each finite element node have to satisfy three conditions, the function value n_{ij} and the values of its derivations $\frac{\partial n_{ij}}{\partial \xi}$ and $\frac{\partial n_{ij}}{\partial \eta}$. After satisfying these conditions, the shape functions are given by the following expressions [15]:

$$\mathrm{n}_{ij} = \mathbf{N}^e \mathbf{a}^e = \mathbf{N}_v^e \mathbf{a}_v^e + \mathbf{N}_u^e \mathbf{a}_u^e \qquad (4)$$

where $\boldsymbol{N}_v^e$ is a matrix of the functions at the finite element nodes, $\boldsymbol{a}_v^e$ is a vector of the displacements at the finite element nodes, while $\boldsymbol{N}_u^e$ and $\boldsymbol{a}_u^e$ are the matrix of additional functions and displacements inside a finite element. Displacements $\boldsymbol{a}_u^e$ are the internal degrees of freedom which can be eliminated at the level of the finite element. After satisfying the conditions at the nodes, three unknown parameters are obtained in the case of the complete polynomial of the fourth order. The shape functions are given in following form:

$$n_{ij} = n^0 + a_1 n^1 + a_2 n^2 + a_3 n^3 \qquad (5)$$

The part of functions n^0 has a unit displacement in the shape functions of translational displacement and a unit rotational angle in the rotational shape functions at the observed nodes, while the displacements and rotations are zero at other nodes. The functions n^1, n^2 and n^3 posses an internal displacement while the displacements and rotations at the nodes are zero.

The shape function of the translational displacement n_{1w}, after satisfying conditions for the function value and the values of its first derivations, is given by the Eq. (6).

Due to the stiffness orthogonality between the additional functions n^1, n^2 and n^3 inside the finite element itself, and also due to the stiffness orthogonality between these functions and functions n^0, it is not possible to influence the solution at the nodes by introducing additional functions. Therefore the shape function of the translational displacement is equal to function n^0 (Eq. (7)).

The shape function of the rotational angle $n_{1\varphi}$, after satisfying conditions for the function value and the values of its first derivations, is given by the Eq. (8).

Between the additional functions, only n^2 is non-orthogonal to the function n^0 and it can be used for improving a numerical solution of the displacement at the nodes. The same conclusion is valid for the shape function $n_{1\theta}$.

In this paper the solution of thin plate problems is analyzed with two types of the shape functions: the shape functions satisfying the homogeneous differential equation of the thin plate bending (SH1) represented by Eqs. (9) and the shape functions with additional mode in the functions of the rotational angle (SH2) represented by Eqs. (10), where the coefficient a is eliminated at the finite element level.

The coefficient a can be determined using global coordinates of the quadrilateral element nodes. Figure 1 shows the transformation of a square element from the local (ξ–η) coordinate system into a rectangular element (Figure 1a) and into an arbitrarily quadrilateral element in the global coordinate system. The local coordinate axis ξ and η divide the rectangular (and parallelogram) into four equal parts with areas A_i=$A/4$, where A_i is an area which belongs to each element node, while A is the area of the whole element. The area A_i is generally different from $A/4$ for the arbitrarily quadrilateral element ($A_i \neq A/4$).

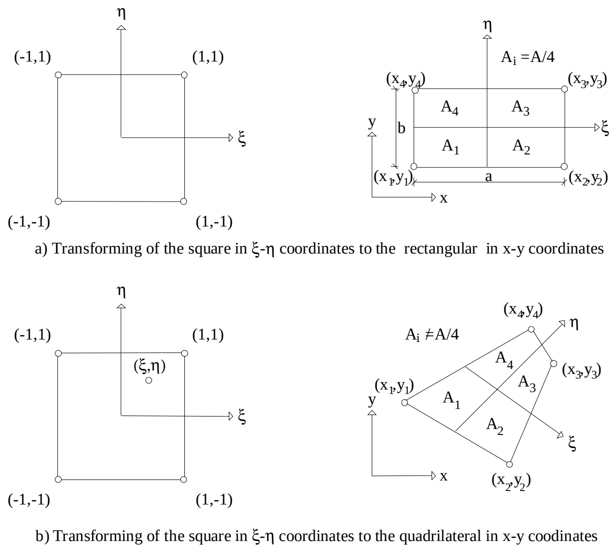

Fig. 1 Transformation of the four-node quadrilateral element

$$\begin{aligned} n_{1w}(\xi,\eta) &= \frac{1}{8}\left(2-3\xi-3\eta+4\xi\eta+\xi^3+\eta^3-\xi^3\eta-\xi\eta^3\right)+ \\ &+\frac{a_{w1}}{8}\left(1-2\xi^2+\xi^4\right)+\frac{a_{w2}}{8}\left(1-\xi^2-\eta^2+\xi^2\eta^2\right)+\frac{a_{w3}}{8}\left(1-2\eta^2+\eta^4\right) \end{aligned} \tag{6}$$

$$n_{1w}(\xi,\eta) = \frac{1}{8}\left(2-3\xi-3\eta+4\xi\eta+\xi^3+\eta^3-\xi^3\eta-\xi\eta^3\right) \tag{7}$$

$$\begin{aligned} n_{1\varphi}(\xi,\eta) &= \frac{1}{8}\left(1-\xi-\eta+\xi\eta-\eta^2+\xi\eta^2+\eta^3-\xi\eta^3\right)+ \\ &+\frac{a_{\varphi 1}}{8}\left(1-2\xi^2+\xi^4\right)+\frac{a_{\varphi 2}}{8}\left(1-\xi^2-\eta^2+\xi^2\eta^2\right)+\frac{a_{\varphi 3}}{8}\left(1-2\eta^2+\eta^4\right) \end{aligned} \tag{8}$$

$$\begin{aligned} n_{1w}(\xi,\eta) &= \frac{1}{8}\left(2-3\xi-3\eta+4\xi\eta+\xi^3+\eta^3-\xi^3\eta-\xi\eta^3\right) \\ n_{1\varphi}(\xi,\eta) &= \frac{1}{8}\left(1-\xi-\eta+\xi\eta-\eta^2+\xi\eta^2+\eta^3-\xi\eta^3\right) \\ n_{1\theta}(\xi,\eta) &= \frac{1}{8}\left(1-\xi-\eta+\xi\eta-\xi^2+\xi^2\eta+\xi^3-\xi^3\eta\right) \end{aligned} \tag{9}$$

$$\begin{aligned} n_{1w}(\xi,\eta) &= \frac{1}{8}\left(2-3\xi-3\eta+4\xi\eta+\xi^3+\eta^3-\xi^3\eta-\xi\eta^3\right) \\ n_{1\varphi}(\xi,\eta) &= \frac{1}{8}\left(1-\xi-\eta+\xi\eta-\eta^2+\xi\eta^2+\eta^3-\xi\eta^3\right)+\frac{a}{8}\left(1-\xi^2-\eta^2+\xi^2\eta^2\right) \\ n_{1\theta}(\xi,\eta) &= \frac{1}{8}\left(1-\xi-\eta+\xi\eta-\xi^2+\xi^2\eta+\xi^3-\xi^3\eta\right)+\frac{a}{8}\left(1-\xi^2-\eta^2+\xi^2\eta^2\right) \end{aligned} \tag{10}$$

Ratio $\frac{A_i}{A/4}$ can be used for improving the approximation of the displacement field and numerical solution for an arbitrarily quadrilateral element. Coefficient a is given by the following expression:

$$a = \frac{1}{4}\sum_{i=1}^{4}\left|1 - \frac{A_i}{A/4}\right| \tag{11}$$

The additional part of the rotational shape functions is multiplied with a half length of the element side 1/2 to ensure unit rotations of the shape functions in the global coordinate system.

If the finite element is rectangular or parallelogram, the value of coefficient a is zero and the shape functions satisfy the homogenous differential equation of the thin plate bending.

3. TRANSFORMATION FROM THE LOCAL TO THE GLOBAL COORDINATE SYSTEM

The equation of the bilinear coordinate transformation is used for transforming the arbitrarily quadrilateral element in the global (x,y) coordinate system into a square element in the local (ξ,η) system (see Figure 1):

$$x = \sum_{i=1}^{4} n_{i0}(\xi,\eta)x_i \; ; \; y = \sum_{i=1}^{4} n_{i0}(\xi,\eta)y_i \tag{12}$$

where:

$$\begin{aligned} &n_{i0} = \frac{1}{4}(1+\xi_i\xi)(1+\eta_i\eta) \\ &(\xi_1,\eta_1)=(-1,-1),\ (\xi_2,\eta_2)=(1,-1), \\ &(\xi_3,\eta_3)=(1,1),\ (\xi_4,\eta_4)=(-1,1) \end{aligned} \tag{13}$$

The shape functions of the four-node finite element are given in the local coordinate system. The second-order Cartesian derivatives in the global coordinate system are necessary to calculate the stiffness matrix element and bending and twisting moments. The first-order Cartesian derivatives can be calculated from the first-order Jacobian matrix. The procedure for calculating the second-order derivatives is presented in this section.

The second-order Cartesian derivatives of the shape functions $n=n(\xi,\eta)$, if $x=x(\xi,\eta)$ and $y=y(\xi,\eta)$ are given in Eqs. (14).

It is not possible to give an explicit expression of ξ and η as a function of x and y. The first-order derivatives $\frac{\partial\xi}{\partial x}$, $\frac{\partial\xi}{\partial y}$, $\frac{\partial\eta}{\partial x}$, $\frac{\partial\eta}{\partial y}$ can be obtained from the first-order Jacobian matrix. The second-order derivatives $\frac{\partial^2\xi}{\partial x^2}$, $\frac{\partial^2\xi}{\partial x\partial y}$, $\frac{\partial^2\xi}{\partial y^2}$, $\frac{\partial^2\eta}{\partial x^2}$, $\frac{\partial^2\eta}{\partial x\partial y}$, $\frac{\partial^2\eta}{\partial y^2}$ cannot be given explicitly. If the mapping from a square element in the local system to a rectangular element in the global system is performed, the second-order derivatives are zero. Therefore the derivatives $\frac{\partial^2 n}{\partial x^2}$, $\frac{\partial^2 n}{\partial y^2}$, $\frac{\partial^2 n}{\partial x\partial y}$ can be easily calculated using the first-order Jacobian matrix.

The mapping of the second-order derivatives form a square element to an arbitrarily quadrilateral element includes the derivation of the functions given in implicit form. The shape functions h are the functions of two variables ξ and η, which are the functions of x and y. Therefore we can write Eqs. (15) and obtain $\frac{\partial n}{\partial x}$, $\frac{\partial n}{\partial y}$ as the functions of ξ, η, $\frac{\partial n}{\partial\xi}$ and $\frac{\partial n}{\partial\eta}$ if the determinant of the first-order Jacobian matrix is different from zero, $|J_1| \neq 0$. The derivatives $\frac{\partial^2 n}{\partial x^2}$ and $\frac{\partial^2 n}{\partial x\partial y}$ can be obtained from the system of Eqs. (16) while the derivatives $\frac{\partial^2 n}{\partial y\partial x}$ and $\frac{\partial^2 n}{\partial y^2}$ can be obtained from Eqs. (17).

The assumption is that $\frac{\partial^2 n}{\partial x\partial y} = \frac{\partial^2 n}{\partial y\partial x}$. The expressions $\frac{\partial}{\partial\xi}\left(\frac{\partial n}{\partial x}\right)$, $\frac{\partial}{\partial\eta}\left(\frac{\partial n}{\partial x}\right)$, $\frac{\partial}{\partial\xi}\left(\frac{\partial n}{\partial y}\right)$ and $\frac{\partial}{\partial\eta}\left(\frac{\partial n}{\partial y}\right)$ are given in Eqs. (18).

$$\begin{aligned}
\frac{\partial^2 n}{\partial x^2} &= \frac{\partial^2 n}{\partial\xi^2}\left(\frac{\partial\xi}{\partial x}\right)^2 + 2\frac{\partial^2 n}{\partial\xi\partial\eta}\frac{\partial\xi}{\partial x}\frac{\partial\eta}{\partial x} + \frac{\partial^2 n}{\partial\eta^2}\left(\frac{\partial\eta}{\partial x}\right)^2 + \frac{\partial n}{\partial\xi}\frac{\partial^2\xi}{\partial x^2} + \frac{\partial n}{\partial\eta}\frac{\partial^2\eta}{\partial x^2} \\
\frac{\partial^2 n}{\partial y^2} &= \frac{\partial^2 n}{\partial\xi^2}\left(\frac{\partial\xi}{\partial y}\right)^2 + 2\frac{\partial^2 n}{\partial\xi\partial\eta}\frac{\partial\xi}{\partial y}\frac{\partial\eta}{\partial y} + \frac{\partial^2 n}{\partial\eta^2}\left(\frac{\partial\eta}{\partial y}\right)^2 + \frac{\partial n}{\partial\xi}\frac{\partial^2\xi}{\partial y^2} + \frac{\partial n}{\partial\eta}\frac{\partial^2\eta}{\partial y^2} \\
\frac{\partial^2 n}{\partial x\partial y} &= \frac{\partial^2 n}{\partial\xi^2}\frac{\partial\xi}{\partial x}\frac{\partial\xi}{\partial y} + \frac{\partial^2 n}{\partial\xi\partial\eta}\left(\frac{\partial\xi}{\partial x}\frac{\partial\eta}{\partial y} + \frac{\partial\xi}{\partial y}\frac{\partial\eta}{\partial x}\right) + \frac{\partial^2 n}{\partial\eta^2}\frac{\partial\eta}{\partial x}\frac{\partial\eta}{\partial y} + \frac{\partial n}{\partial\xi}\frac{\partial^2\xi}{\partial x\partial y} + \frac{\partial n}{\partial\eta}\frac{\partial^2\eta}{\partial x\partial y}
\end{aligned} \tag{14}$$

$$\frac{\partial n}{\partial \xi}=\frac{\partial n}{\partial x}\frac{\partial x}{\partial \xi}+\frac{\partial n}{\partial y}\frac{\partial y}{\partial \xi} \quad ; \quad \frac{\partial n}{\partial \eta}=\frac{\partial n}{\partial x}\frac{\partial x}{\partial \eta}+\frac{\partial n}{\partial y}\frac{\partial y}{\partial \eta} \tag{15}$$

$$\frac{\partial\left(\frac{\partial n}{\partial x}\right)}{\partial \xi}=\frac{\partial^2 n}{\partial x^2}\frac{\partial x}{\partial \xi}+\frac{\partial^2 n}{\partial x \partial y}\frac{\partial y}{\partial \xi} \quad ; \quad \frac{\partial\left(\frac{\partial n}{\partial x}\right)}{\partial \eta}=\frac{\partial^2 n}{\partial x^2}\frac{\partial x}{\partial \eta}+\frac{\partial^2 n}{\partial x \partial y}\frac{\partial y}{\partial \eta} \tag{16}$$

$$\frac{\partial\left(\frac{\partial n}{\partial y}\right)}{\partial \xi}=\frac{\partial^2 n}{\partial y \partial x}\frac{\partial x}{\partial \xi}+\frac{\partial^2 n}{\partial y^2}\frac{\partial y}{\partial \xi} \quad ; \quad \frac{\partial\left(\frac{\partial n}{\partial y}\right)}{\partial \eta}=\frac{\partial^2 n}{\partial y \partial x}\frac{\partial x}{\partial \eta}+\frac{\partial^2 n}{\partial y^2}\frac{\partial y}{\partial \eta} \tag{17}$$

$$\begin{aligned}
\frac{\partial}{\partial \xi}\left(\frac{\partial n}{\partial x}\right)&=\frac{\partial^2 n}{\partial \xi^2}\frac{\partial \xi}{\partial x}+\frac{\partial n}{\partial \xi}\frac{\partial \eta}{\partial x}\left(-\frac{\partial^2 x}{\partial \xi \partial \eta}\frac{\partial \xi}{\partial x}-\frac{\partial^2 y}{\partial \xi \partial \eta}\frac{\partial \xi}{\partial y}\right)+\frac{\partial^2 n}{\partial \xi \partial \eta}\frac{\partial \eta}{\partial x}+\frac{\partial n}{\partial \eta}\frac{\partial \eta}{\partial x}\left(-\frac{\partial^2 x}{\partial \xi \partial \eta}\frac{\partial \eta}{\partial x}-\frac{\partial^2 y}{\partial \xi \partial \eta}\frac{\partial \eta}{\partial y}\right)\\
\frac{\partial}{\partial \eta}\left(\frac{\partial n}{\partial x}\right)&=\frac{\partial^2 n}{\partial \xi \partial \eta}\frac{\partial \xi}{\partial x}+\frac{\partial n}{\partial \xi}\frac{\partial \xi}{\partial x}\left(-\frac{\partial^2 x}{\partial \xi \partial \eta}\frac{\partial \xi}{\partial x}-\frac{\partial^2 y}{\partial \xi \partial \eta}\frac{\partial \xi}{\partial y}\right)+\frac{\partial^2 n}{\partial \eta^2}\frac{\partial \eta}{\partial x}+\frac{\partial n}{\partial \eta}\frac{\partial \xi}{\partial x}\left(-\frac{\partial^2 x}{\partial \xi \partial \eta}\frac{\partial \eta}{\partial x}-\frac{\partial^2 y}{\partial \xi \partial \eta}\frac{\partial \eta}{\partial y}\right)\\
\frac{\partial}{\partial \xi}\left(\frac{\partial n}{\partial y}\right)&=\frac{\partial^2 n}{\partial \xi^2}\frac{\partial \xi}{\partial y}+\frac{\partial n}{\partial \xi}\frac{\partial \eta}{\partial y}\left(-\frac{\partial^2 x}{\partial \xi \partial \eta}\frac{\partial \xi}{\partial x}-\frac{\partial^2 y}{\partial \xi \partial \eta}\frac{\partial \xi}{\partial y}\right)+\frac{\partial^2 n}{\partial \xi \partial \eta}\frac{\partial \eta}{\partial y}+\frac{\partial n}{\partial \eta}\frac{\partial \eta}{\partial y}\left(-\frac{\partial^2 x}{\partial \xi \partial \eta}\frac{\partial \eta}{\partial x}-\frac{\partial^2 y}{\partial \xi \partial \eta}\frac{\partial \eta}{\partial y}\right)\\
\frac{\partial}{\partial \eta}\left(\frac{\partial n}{\partial y}\right)&=\frac{\partial^2 n}{\partial \xi \partial \eta}\frac{\partial \xi}{\partial y}+\frac{\partial n}{\partial \xi}\frac{\partial \xi}{\partial y}\left(-\frac{\partial^2 x}{\partial \xi \partial \eta}\frac{\partial \xi}{\partial x}-\frac{\partial^2 y}{\partial \xi \partial \eta}\frac{\partial \xi}{\partial y}\right)+\frac{\partial^2 n}{\partial \eta^2}\frac{\partial \eta}{\partial y}+\frac{\partial n}{\partial \eta}\frac{\partial \xi}{\partial y}\left(-\frac{\partial^2 x}{\partial \xi \partial \eta}\frac{\partial \eta}{\partial x}-\frac{\partial^2 y}{\partial \xi \partial \eta}\frac{\partial \eta}{\partial y}\right)
\end{aligned} \tag{18}$$

Finally, the second-order Cartesian derivatives $\frac{\partial^2 n}{\partial x^2}$, $\frac{\partial^2 n}{\partial y^2}$ and $\frac{\partial^2 n}{\partial x \partial y}$ can be calculated by solving the system of equations (16) and (17).

The described procedure can be given in the matrix form as follows. The relation between the first-order derivatives of the shape function *n* in the local and global coordinates is:

$$\begin{Bmatrix} \frac{\partial n}{\partial \xi} \\ \frac{\partial n}{\partial \eta} \end{Bmatrix} = \boldsymbol{J}_1 \begin{Bmatrix} \frac{\partial n}{\partial x} \\ \frac{\partial n}{\partial y} \end{Bmatrix} \tag{19}$$

where $\boldsymbol{J_1}$ is the first-order Jacobian matrix:

$$\boldsymbol{J}_1 = \begin{bmatrix} \frac{\partial x}{\partial \xi} & \frac{\partial y}{\partial \xi} \\ \frac{\partial x}{\partial \eta} & \frac{\partial y}{\partial \eta} \end{bmatrix} \tag{20}$$

The relation between the second-order derivatives is:

$$\begin{Bmatrix} \frac{\partial^2 n}{\partial \xi^2} \\ \frac{\partial^2 n}{\partial \eta^2} \\ \frac{\partial^2 n}{\partial \xi \eta} \end{Bmatrix} = \boldsymbol{J}_2 \begin{Bmatrix} \frac{\partial^2 n}{\partial x^2} \\ \frac{\partial^2 n}{\partial y^2} \\ \frac{\partial^2 n}{\partial x \partial y} \end{Bmatrix} + \begin{Bmatrix} 0 \\ 0 \\ \alpha \frac{\partial n}{\partial x} + \beta \frac{\partial n}{\partial y} \end{Bmatrix} \tag{21}$$

where $\boldsymbol{J_2}$ is the second-order Jacobian matrix:

$$\boldsymbol{J}_2 = \begin{bmatrix} \left(\frac{\partial x}{\partial \xi}\right)^2 & \left(\frac{\partial y}{\partial \xi}\right)^2 & 2\frac{\partial x}{\partial \xi}\frac{\partial y}{\partial \xi} \\ \left(\frac{\partial x}{\partial \eta}\right)^2 & \left(\frac{\partial y}{\partial \eta}\right)^2 & 2\frac{\partial x}{\partial \eta}\frac{\partial y}{\partial \eta} \\ \frac{\partial x}{\partial \xi}\frac{\partial x}{\partial \eta} & \frac{\partial y}{\partial \xi}\frac{\partial y}{\partial \eta} & \frac{\partial x}{\partial \xi}\frac{\partial y}{\partial \eta}+\frac{\partial y}{\partial \xi}\frac{\partial x}{\partial \eta} \end{bmatrix} \tag{22}$$

while α and β are coefficients which depend on the global coordinate of the finite element nodes:

$$\begin{aligned} \alpha &= \frac{\partial^2 x}{\partial \xi \partial \eta} = \sum_{i=1}^{4} \frac{\xi_i \eta_i}{4} x_i = \frac{1}{4}\left(x_1 - x_2 + x_3 - x_4\right) \\ \beta &= \frac{\partial^2 y}{\partial \xi \partial \eta} = \sum_{i=1}^{4} \frac{\xi_i \eta_i}{4} y_i = \frac{1}{4}\left(y_1 - y_2 + y_3 - y_4\right) \end{aligned} \tag{23}$$

The determinant of the second-order Jacobian matrix is:

$$\left|\boldsymbol{J}_2\right| = \left(\frac{\partial x}{\partial \xi}\frac{\partial y}{\partial \eta} - \frac{\partial x}{\partial \eta}\frac{\partial y}{\partial \xi}\right)^3 = \left|\boldsymbol{J}_1\right|^3 \tag{24}$$

When $\left|J_2\right| \neq 0$, the inverse matrix of the second-order Jacobian matrix is:

$$\boldsymbol{J}_2^{-1} = \frac{1}{|\boldsymbol{J}_1|^2}\begin{bmatrix} \left(\frac{\partial y}{\partial \eta}\right)^2 & \left(\frac{\partial y}{\partial \xi}\right)^2 & -2\frac{\partial y}{\partial \xi}\frac{\partial y}{\partial \eta} \\ \left(\frac{\partial x}{\partial \eta}\right)^2 & \left(\frac{\partial x}{\partial \xi}\right)^2 & -2\frac{\partial x}{\partial \xi}\frac{\partial x}{\partial \eta} \\ -\frac{\partial x}{\partial \eta}\frac{\partial y}{\partial \eta} & -\frac{\partial x}{\partial \xi}\frac{\partial y}{\partial \xi} & \frac{\partial x}{\partial \xi}\frac{\partial y}{\partial \eta}+\frac{\partial x}{\partial \eta}\frac{\partial y}{\partial \xi} \end{bmatrix} \tag{25}$$

Finally, the second-order Cartesian derivatives are:

$$\begin{Bmatrix} \frac{\partial^2 n}{\partial x^2} \\ \frac{\partial^2 n}{\partial y^2} \\ \frac{\partial^2 n}{\partial x \partial y} \end{Bmatrix} = \boldsymbol{J}_2^{-1}\begin{Bmatrix} \frac{\partial^2 n}{\partial \xi^2} \\ \frac{\partial^2 n}{\partial \eta^2} \\ \frac{\partial^2 n}{\partial \xi \partial \eta} - \alpha' \frac{\partial n}{\partial \xi} + \beta' \frac{\partial n}{\partial \eta} \end{Bmatrix} \tag{26}$$

where:

$$\alpha' = \frac{1}{|\boldsymbol{J}_1|}\left(\alpha\frac{\partial y}{\partial \eta} - \beta\frac{\partial x}{\partial \eta}\right); \ \beta' = \frac{1}{|\boldsymbol{J}_1|}\left(\alpha\frac{\partial y}{\partial \xi} - \beta\frac{\partial x}{\partial \xi}\right) \tag{27}$$

If the finite element is a parallelogram, the values of coefficients are $\alpha'=\beta'=0$.

4. NUMERICAL EXAMPLES

The four-node plate element with independent translational and rotational DOF is tested on a few examples. The results of the computation are compared with the analytical solution and also with those obtained with some other plate finite elements.

4.1 Bending of square plate - rectangular elements

A simply supported, clamped and corner supported square homogeneous isotropic plate with a side length *a*, subjected to the uniformly distributed load *p* and the central concentrated load *P*, is analyzed.

The central deflection and the central bending moment computed with the element developed in this paper are represented in Tables 1-3 for several meshes. The numerical solutions of the deflection and the bending moment converge to the exact solution for all subdivisions with the increase of the degrees of freedom. The accuracy of the numerical solution of the deflection is higher than the accuracy of the bending moment which is a characteristic of the displacement method.

Table 1 A square plate uniformly loaded, ν=0.3

Mesh	Simply supported plate		Clamped plate	
	w	M_y	w	M_y
2×2	0.004185	0.06990	0.001447	0.04514
4×4	0.004076	0.05048	0.001374	0.02799
8×8	0.004066	0.04850	0.001295	0.02406
12×12	0.004064	0.04816	0.001279	0.02341
16×16	0.004062	0.04801	0.001270	0.02318
Exact [16]	0.004062	0.04790	0.001260	0.02310
Multiplier	pa^4/D	pa^2	pa^4/D	pa^2

Table 2 A square plate with a concentrated central load, ν=0.3

Mesh	Simply supported plate		Clamped plate	
	w	M_y	w	M_y
2×2	0.01389	0.2478	0.00625	0.1950
4×4	0.01220	0.3017	0.00615	0.2511
8×8	0.01180	0.3731	0.00577	0.3199
12×12	0.01170	0.4138	0.00569	0.3602
16×16	0.01165	0.4436	0.00566	0.3899
Exact [16]	0.01160	-	0.00559	-
Multiplier	Pa^2/D	Pa^2	Pa^2/D	Pa^2

The numerical displacements for *16×16* mesh are compared with the exact solutions. The maximum displacement discrepancy is *1.25%* for a clamped plate with a concentrated central load. The discrepancy in other examples is lower, while the deflection for a simply supported uniformly loaded plate is equal to the exact for *16×16* mesh.

Table 3 Corner supported square plate with a uniform load p, ν=0.3

Mesh	Number of elements	Number of nodes	Point 1		Point 2	
			w	M_y	w	M_y
4x4	16	25	0.0165	0.1478	0.0262	0.1103
8x8	64	81	0.0171	0.1497	0.0277	0.1114
16x16	256	289	0.0173	0.1498	0.0280	0.1114
Exact (Marcus) [17]			0.0180	0.154	0.0281	0.110
Exact (Ballesteros, Lee) [18]			0.0170	0.140	0.0265	0.109
Multiplier			pa^4/D	pa^2	pa^4/D	pa^2
Note: Point 1- center of side, Point 2 - center of plate						

The error of the numerical solutions for the corner supported plate deflection is 0.35% with respect to the exact solution [17], while the error of the bending moment is *1.27%*.

The errors of the central deflection w_c of a simply supported and clamped square plate with a uniform load are compared in Figures 2 and 3 with various rectangular elements. The results for comparing the error are taken from Ref. [19]. The analyzed elements are: ACM (Zienkiewicz, Cheung - displacement non-conforming), Q19 (Clough, Felippa - displacement conforming), M (Fraejis de Veubeke - equilibrium), DKQ (Batoz, Ben Tohar - discrete Kirchhoff), HTQ3 (Jirousek, Lan Guex - hibrid), H5 (Cook - hibrid) and TP-SF1 (element presented in this paper with shape functions satisfying a homogeneous differential equation of the thin plate bending).

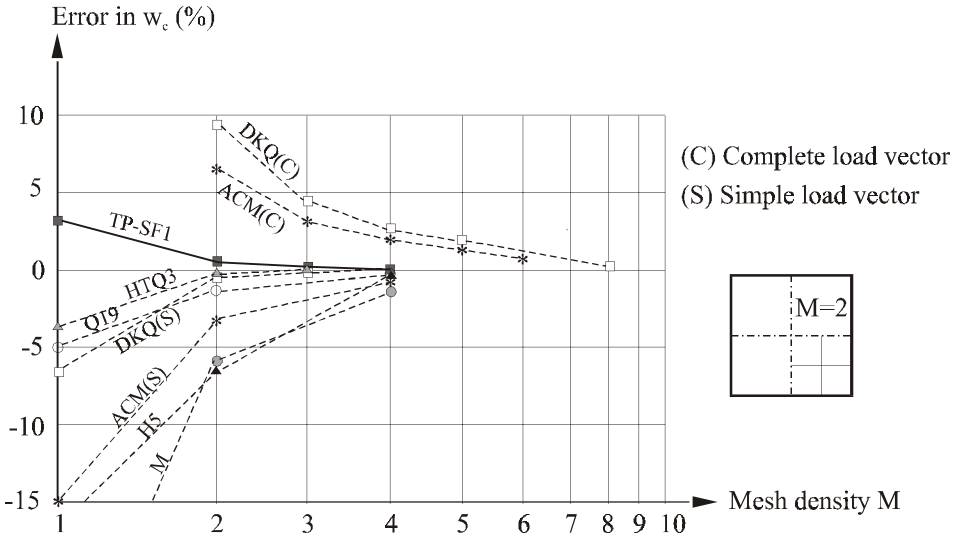

Fig. 2 The central displacement error for a simply supported uniformly loaded square plate

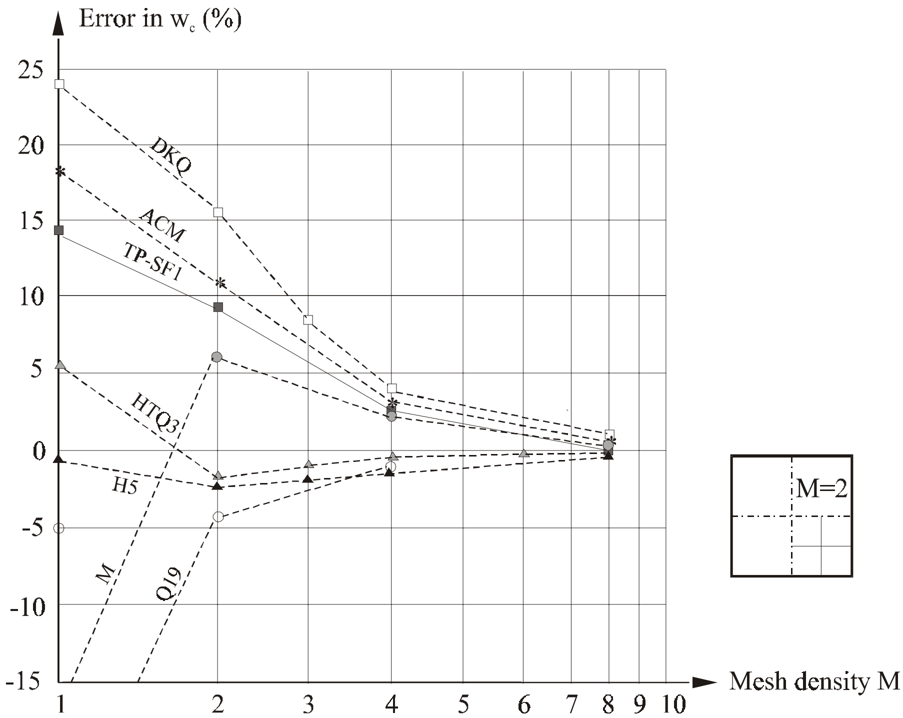

Fig. 3 The central displacement error for uniformly loaded clamped square plate

4.2 Twisted ribbon - single element test

The twisted ribbon is a test that shows the effect of the element aspect ratio. The twisting moment is applied by corner couples or by corner moments as shown in Figure 4. The plate is usually modeled by one rectangular element. Benchmark values were obtained from a mesh of 16 rectangular Kirchhoff elements with 16 DOF each. Many types of elements fail this test.

The two loadings produce the same displacement for the element proposed in this paper. The obtained solution is compared in Figure 5 with solutions obtained with one discrete Kirchhoff quadrilateral element [20] and with benchmark values (16 Kirchhoff elements with 16 DOF) [20].

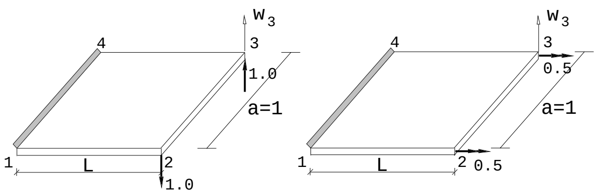

Fig. 4 Twisted ribbon, ν=0.25

It is shown that the increase of the ratio of the rectangular element sides has no influence on the solution in this example.

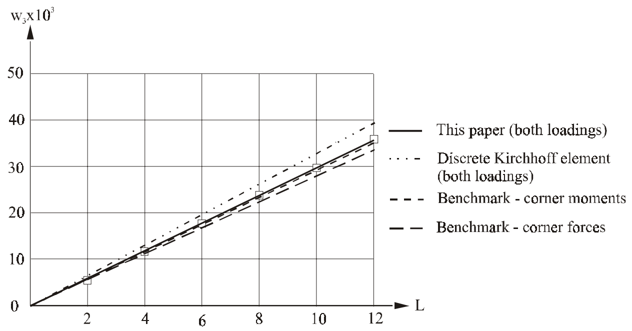

Fig. 5 Deflection of the twisted ribbon

4.3 A skew simply supported plate

A skew simply supported plate with a uniformly distributed load is analyzed. The discretization of the plate is shown in Figure 6. The results of the central deflection and central bending moment are given in Table 4 and compared with the exact solution [21].

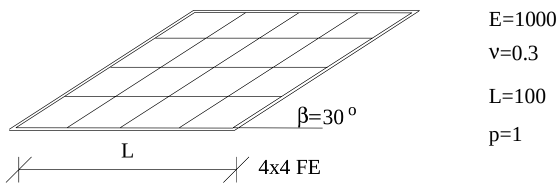

Fig. 6 A skew simply supported plate under uniform load

Table 4 A skew simply supported plate under uniform load

Mesh	$w \cdot c_1$	$M_x \cdot c_2$	$M_y \cdot c_2$
4x4	*0.3480*	*1.532*	*0.786*
8x8	*0.3819*	*1.804*	*1.036*
16x16	*0.3938*	*1.838*	*1.077*
32x32	*0.3981*	*1.860*	*1.078*
Q4BL(32x32) [10]	*0.42352*	*1.953*	*1.140*
Exact - Morley [21]	*0.40800*	*1.910*	*1.080*
Multiplier	$c_1=pa^4/1000D$	$c_2=pa^2/100$	$c_2=pa^2/100$

It is shown that the numerical solution converges to the exact one [21] with the increase of the degrees of freedom. The error of the deflection for *32×32* mesh is -2.4% with respect to the exact solution, while the error of the bending moment is -2.6 for M_x and -0.2% for M_y. The results are also compared to those obtained by a quadrilateral four-node finite element Q4BL [10] for *32×32* mesh.

4.4 Bending of square plate - quadrilateral elements

A simply supported square plate under the uniformly distributed load *p* is analyzed using quadrilateral elements. Two different meshes shown in Figure 7 and two shape functions (SF1 - satisfying homogeneous differential equations and SF2 - shape functions of rotational angle with additional mode) are used to assess the effect of mesh distortion on the accuracy.

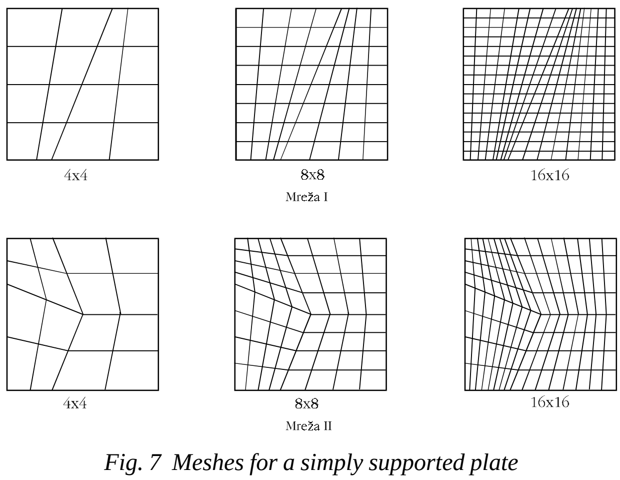

Fig. 7 Meshes for a simply supported plate

Table 5 Square plate uniformly loaded, w/w_{anal}, ν=0.3

Mesh	*Number of d.o.f.*	*Mesh I*		*Mesh II*	
		SF1	*SF2*	*SF1*	*SF2*
4x4	*75*	*0.959*	*1.015*	*0.963*	*1.025*
8x8	*243*	*0.973*	*1.007*	*0.960*	*1.014*
16x16	*867*	*0.983*	*1.005*	*0.958*	*1.012*

The numerical solution of the deflection is shown in Table 5. The central deflection error of the plate is analyzed for 16×16 finite elements. The shape functions SF1 give the central deflection error of -1.7% for mesh I and -4.2% for mesh II . The error obtained with SF2 is 0.5% for mesh I and 1.2% for mesh II. It is shown that the introduction of additional modes in the shape functions of the rotational angle improves the numerical solution in arbitrarily quadrilateral elements.

5. CONCLUSIONS

An arbitrarily quadrilateral thin plate finite element with independent translational and rotational degrees of freedom and different shape functions for the approximation of the displacement and rotations has been presented. Two types of the shape functions are analyzed: the shape functions which satisfy the homogeneous differential equation of the thin plate bending and the shape functions with additional internal modes in the functions of rotational angle which depend on the finite element geometry. The procedure for transforming the second-order derivatives of the shape functions from the local to the global coordinate system, which is necessary for evaluating the strain and the stiffness matrix, is developed. Several examples are analyzed to show the quality of the numerical solution. The numerical solution in examples with regular discretization (square and rectangular finite elements) converges very fast to the exact solution. Increasing the ratio of rectangular element sides has no influence on the numerical solution. The convergence of the numerical solution for discretization with a parallelogram and arbitrarily quadrilateral finite elements is also achieved. It was shown that the additional modes in the shape functions of the rotational angle improve a solution for discretization with arbitrarily quadrilateral elements.

6. ACKNOWLEDGMENTS

Partial financial support, provided by the Ministry of Science and Technology of the Republic of Croatia under the project Non-linear Stability and Bearing Capacity of Frames and Plate Structures, Grant No. 0083051, is gratefully acknowledged.

7. REFERENCES

[1] M.M. Hrabok and T. M. Hrudey, A rewiew and catalogue of plate bending finite elements, *Computers & Structures*, Vol. 19, pp. 474-498, 1984.

[2] O.C. Zienkiewicz and R.L. Taylor, *The Finite Element Method: Solid Mechanics*, 5th ed., Vol. II, Butterworth-Heinemann, Oxford, 2000.

[3] R.J. Melosh, A stiffness matrix for the analysis of thin plates in bending, *J. Aeronaut Sci*, Vol. 28, No. 34, 1961.

[4] O.C. Zienkiewicz and Y.K. Cheung, The finite element method for analysis of elastic isotropic and ortotropic slabs, Proc. Inst. Civ. Eng., Vol. 28, pp. 471-488, 1964.

[5] T.H.H. Pian and P. Tong, Rationalization in deriving element stiffness matrices by assumed stress approach, Proc. 2nd Conf. on Matrix Meth. in Struct. Mech., pp. 441-469, 1969.

[6] J.L. Batoz and M.B. Tahar, Evaluation of a new quadrilateral thin plate bending element, *Int. J. Num. Meth. Eng.*, Vol. 18, pp. 1655-1677, 1982.

[7] Y. Long, X. Bu, Z. Long and Y. Xu, Generalized conforming plate bending elements using point and line compatibility conditions, *Computers & Structures*, Vol. 54, No. 4, pp. 717-723, 1995.

[8] C. Wanji and Y.K. Cheung, Refined non-conforming quadrilateral thin plate bending element, *Int. J. Num. Meth. Eng.*, Vol. 40, pp. 391-935, 1997.

[9] M.A. Crisfield, *Non-linear Finite Element Analysis of Solids and Structures*, Vol. 1, John Wiley, Chichester, Sussex, 1991.

[10] O.C. Zienkiewicz, Z. Xu, L.F. Zeng, A. Samuelsson and N.E. Wiberg, Linked interpolation for Reissner-Mindlin plate elements: part I - a simple quadrilateral element, *Int. J. Num. Meth. Eng.*, Vol. 36, pp. 304-356, 1993.

[11] Z. Xu, O.C. Zienkiewicz, L.F. Zeng, A. Samuelsson and N.E. Wiberg, Linked interpolation for Reissner-Mindlin plate elements: part III - an alternative quadrilateral, *Int. J. Num. Meth. Eng.*, Vol. 37, pp. 143-743, 1994.

[12] F. Auricchio and R.L. Taylor, A shear deformable plate element with an exact thin limit, *Comp. Meth. Appl. Mech. Eng*, Vol. 118, pp. 393-412, 1994.

[13] A. Ibrahimbegović, A unified formulation for modelling of structural system: finite elements with rotational degrees of freedom, *Int. J. Engineering Modelling*, Vol. 3, No. 1-2, pp. 21-27, 1990.

[14] A. Mihanović, V. Herak-Marović and P. Marović, The formulation of new fully compatible quadrilateral shell finite element, *Int. J. Engineering Modelling*, Vol. 6, No. 1-4, pp. 1-11, 1993.

[15] Ž. Nikolić, Contribution to the improvement of solutions on finite elements in frame structures and thin plates, Ph. D. Thesis, Faculty of Civil Engineering, University of Split, 1999. (in Croatian)

[16] S.P. Timoshenko and S. Woinowsky-Krieger, *Theory of Plates and Shells*, 2nd ed., McGraw-Hill, New York, 1959.

[17] H. Marcus, *Die Theorie elastisher Gewebe und ihre Anwendung auf die Berechnung biegsamer Platten*, Springer, Berlin, 1932.

[18] P. Ballesteros and S.L. Lee, Uniformly loaded rectangular plate supported at the corners, *Int. J. Mech. Sci.*, No. 2, pp. 206-211, 1960.

[19] O.C. Zienkiewicz and R.L. Taylor, *The Finite Element Method: Basic Formulation and Linear Problems*, 4th ed., Vol. 1, McGraw-Hill, London, 1989.

[20] R. Cook, D.S. Malkus and M.E. Plesha, *Concepts and Applications of Finite Element Analysis*, 3rd ed., John Wiley & Sons, 1989.

[21] L.S.D. Morley, *Skew Plates and Structures*, International Series of Monographs in Aeronautics and Astronautics, Macmillan, New York, 1963.

ČETVEROČVORNI KONAČNI ELEMENT TANKE PLOČE S NEZAVISNIM ROTACIJSKIM STUPNJEVIMA SLOBODE

SAŽETAK

U ovome radu prikazan je četveročvorni potpuno kompatibilan konačni element za analizu savijanja tankih ploča. Upotrijebljeni element ima nezavisne translacijske i rotacijske stupnjeve slobode u svakom čvoru. Bazne funkcije za aproksimaciju polja pomaka i zaokreta su različite, a jedne i druge se određuju iz potpunog polinoma četvrtog stupnja. Nakon zadovoljenja uvjeta za vrijednost funkcije i njenih prvih derivacija u čvorovima, bazne funkcije se sastoje od nepromjenljivog dijela koji zadovoljava homogenu diferencijalnu jednadžbu ploče i dodatnog promjenljivog dijela. Nepromjenljivi dio osigurava visoku točnost rješenja za konačne elemente s paralelnim nasuprotnim stranicama (pravokutnik, paralelogram). Dodatni promjenjivi dijelovi u baznim funkcijama kuteva zaokreta mogu se upotrijebiti za poboljšanje rješenja kod mreže nepravilnih četveročvornih elemenata. Opisani postupak osigurava visok red interpolacije polja pomaka ploče. U oba slučaja konačni element ima 12 stupnjeva slobode. Dodatne nepoznanice u baznim funkcijama zaokreta eliminiraju se na nivou elementa.

Ključne riječi: tanka ploča, *četveročvorni konačni element, nezavisni rotacijski stupnjevi slobode.*